HiSTGNN: Hierarchical Spatio-temporal Graph Neural Networks for Weather Forecasting

Minbo Ma, Peng Xie, Fei Teng,Tianrui Li, *Senior Member, IEEE,*
Bin Wang, Shenggong Ji, and Junbo Zhang, *Member, IEEE,*

Abstract—Weather Forecasting is an attractive challengeable task due to its influence on human life and complexity in atmospheric motion. Supported by massive historical observed time series data, the task is suitable for data-driven approaches, especially deep neural networks. Recently, the Graph Neural Networks (GNNs) based methods have achieved excellent performance for spatio-temporal forecasting. However, the canonical GNNs-based methods only individually model the local graph of meteorological variables per station or the global graph of whole stations, lacking information interaction between meteorological variables in different stations. In this paper, we propose a novel Hierarchical Spatio-Temporal Graph Neural Network (HiSTGNN) to model cross-regional spatio-temporal correlations among meteorological variables in multiple stations. An adaptive graph learning layer and spatial graph convolution are employed to construct self-learning graph and study hidden dependency among nodes of variable-level and station-level graph. For capturing temporal pattern, the dilated inception as the backbone of gate temporal convolution is designed to model long and various meteorological trends. Moreover, a dynamic interaction learning is proposed to build bidirectional information passing in hierarchical graph. Experimental results on three real-world meteorological datasets demonstrate the superior performance of HiSTGNN beyond 7 baselines and it reduces the errors by 4.2% to 11.6% especially compared to state-of-the-art weather forecasting method.

Index Terms—Weather forecasting, Spatio-temporal data mining, Hierarchical Graph Neural Networks

1 Introduction

Meteorological variables, like temperature, wind speed and humidity, have a profound impact on many aspects of human livelihood such as transportation, agriculture, industry, etc [1]. They also play a fundamental role in interdisciplinary research by providing auxiliary information support. Taking traffic prediction in urban computing research as an example, the volume and speed of traffic are closely related to the current weather conditions [2].

Weather forecasting aims to present accurate and timely predictions of meteorological variables in advance, which plays directive role in planning of daily living and production activities. Taking the heating in the winter as an example, suppose heating department is aware of future temperature ahead of time, it can rationalize the intensity of heating to prevention of unnecessary energy consumption. In this paper, we simultaneously predict multiple meteorological variables for multiple weather stations over multiple future time steps called 3M task. It is very challenging due to the following two complex factors: 1) *Multiple spatio-temporal correlations among meteorological variables.* First, weather forecasting is a typical time-series forecasting task in which each variable has a corresponding temporal pattern.Then we notice that variables are tightly coupled. For instance, the temperature and atmosphere pressure follow proportional relation under consideration in thermal theory. In addition, Such relation is bidirectional and asymmetric, and difficult to quantify or express in formulas. Not only local meteorological variables (i.e., generated from the same weather station) are correlated, but also those in geographical neighborhoods (i.e. spatially adjacent weather stations), due to the dynamics of Earth's atmospheric system. As an example

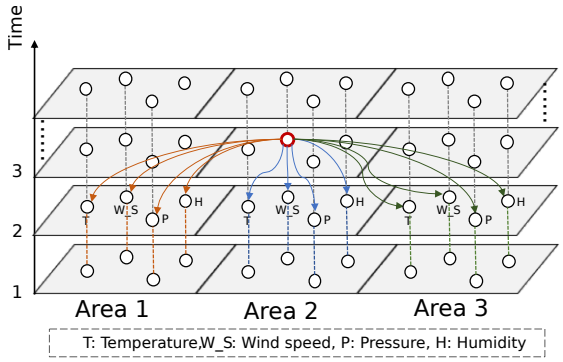

Fig. 1. Illustration of multiple spatio-temporal correlations among meteorological variables.

- *Minbo Ma, Peng Xie, Fei Teng and Tianrui Li (the corresponding author) are with School of Computing and Artifical Intelligence, Southwest Jiaotong University, Chengdu 611756, China. Tianrui Li is also with National Enginnering Laboratory of Integrated Transportation Big Data Application Technology. E-mails: minboma@my.swjtu.edu.cn, pengxie@my.swjtu.edu.cn, fteng@swjtu.edu.cn, trli@swjtu.edu.cn.*
- *Bin Wang is with the School of Computer Science and Technology, Ocean University of China, Qingdao 266100, China. E-mail: wangbin9545@ouc.edu.cn.*
- *Shenggong Ji is with Tencent Inc., Shenzhen, China. E-mail: shenggongji@163.com.*
- *Junbo Zhang is with JD iCity, JD Technology, JD Intelligent Cities Research, Beijing, China. E-mail: msjunbozhang@outlook.com.*

Manuscript received xxx xx, xxxx; revised xxxx xx, xxxx.

(see Fig. 1), to predict the wind speed at the time point t_3, it is necessary to utilize the previous information of wind speed in area 2 and other variables in same area as well as adjacent areas. Thus, to present accurate weather forecasting, we need to consider both the spatio-temporal correlations among meteorological variables in each area and adjacent areas. 2) *Complex spatial dependencies among stations*. The weather stations which are geographically distant from each other, following similar temporal pattern among meteorological variables, may have strong correlation influenced by terrain, topography, or atmospheric circulation, etc.

Numerical Weather Prediction (NWP) is currently the common method for weather forecasting, which obtains prediction by solving nonlinear differential equations accounting for atmospheric dynamics. However, NWP may be imprecise limited by the current theory of atmospheric physics and inappropriate choice of initial solution for differential equations [3]. Moreover, the computing resources require for NWP is enormous. Supported by the tremendous amounts of observed meteorological data, researchers introduce data-driven methods to tackle the weather forecasting task [4], [5], [6]. Among these methods, Deep Learning (DL) based approaches achieve the desirable performance by using neural networks to learn the meteorological changing patterns and avoid the tedious feature engineering of traditional machine learning methods. However, the majority of DL-based methods only consider capturing temporal or spatio-temporal dependencies of meteorological variables for each weather station, but completely neglect or implicitly model the complicated spatial interaction among stations.

To tackle aforementioned challenges, we propose a **Hi**erarchical **S**patio-**T**emporal **G**raph **N**eural **N**etworks (HiSTGNN, see Fig. 3) for multi-step weather forecasting of multiple meteorological variables across multiple weather stations. First, we observe that hierarchical graph structure is well suited for capturing the correlation between different levels. Inspired by this perspective, we introduce the hierarchical spatial graph (see Fig. 2(a)) in which a station is seen as a hypernode (i.e., the node containing a subgraph) and a variable is seen as a node of the corresponding station. Fig. 2(b) depicts an illustration of hierarchical spatio-temporal graph which stacks hierarchical spatial graphs along the time axis.

Based on this hierarchical view, we design the spatio-temporal learning module with dilated inception network and graph convolutional network to capture the spatial and temporal dependencies of variable level and station level, respectively. Considering that there is not explicit graph structure among variables and the incompleteness relationship among stations, the adaptive graph learning module studies graph structure in the form of graph adjacency matrix from observed data. In particular, uni-directed edge is to model the asymmetric relation inter-variable and inter-station. Besides, to capture the global weather station context for the local meteorological variable modeling, the dynamic interaction learning module is designed to aggregates representation of the local graph into the corresponding global node and diffuse information in inverse direction. To summarize, our contributions are as follows:

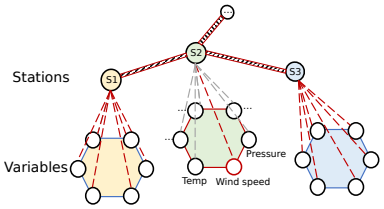

(a) Hierarchical spatial graph.

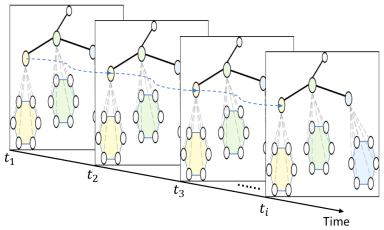

(b) Hierarchical spatio-temporal graph

Fig. 2. Modeling multiple spatio-temporal correlation from a hierarchical perspective. In (a), the red line indicates the route that red node (wind speed variable) is associated with others in current station and adjacent stations.

- We propose a hierarchical spatio-temporal graph neural network to model the spatial correlations and temporal dependencies among meteorological variables of local weather station and global stations in an end-to-end manner.
- We design a generic dynamic interaction learning module to establish bidirectional message passing between the station-level graph and variable-level graphs with an iterative framework.
- We evaluate our method on on three real-world weather datasets. The experimental results show that our HiSTGNN achieves the state-of-the-art performance beyond 7 baselines which includes CNN/RNN/GNN and traditional time series methods.

The rest of the paper is organized as follows. We first review related works in Section 5 and introduce the formulation of the multi-station weather forecasting problem in Section 2. Then we present the details of our method in Section 3. We discuss experiments and performance analysis in Section 4. Last, we conclude our work in Section 6.

2 Problem Formulation

In this paper, we formalize the task of weather forecasting as spatio-temporal forecasting of multiple weather stations, multiple meteorological variables and multiple steps. We first present the definitions of hierarchical spatio-temporal graph. Next, we give the problem statement and corresponding notions.

2.1 Definitions

As illustrated in Fig. 2(a), in this study, we cast weather stations and meteorological variables as nodes of a hierarchical graph, which consists of multiple local graphs and a global graph. We give the formal definitions of spatio-temporal hierarchical graph-related concepts as follows:

Definition 1. Local Graph. A local graph represents *variable-level graph* of single weather station, denoted as $G_l = (V_l, E_l)$ where V_l is the set of meteorological variables, and E_l is the set of relationships of paired variables.

Definition 2. Global Graph. Let $G_g = (V_g, E_g)$ denotes the global graph, i.e. *station-level graph*. The weather stations are defined as V_g, and the relationships of paired stations are defined as E_g.

Definition 3. Hierarchical spatio-temporal graph. Let $\mathcal{G}^t = \{G_l^t, G_g^t | G_l^t = (V, E_t, W_t), G_l^t = (V, E_t, W_t)\}$ denotes the hierarchical graph at time step t (as shown Fig. 2(b)). Here, W_t represents the dynamic features of nodes and its values varies with time, which is analogous to the changing process of meteorological variables.

Definition 4. Node Neighborhood. Let $e = (v_i, v_j) \in E$ denotes that there is an edge between the node v_i and the node v_j. The neighborhood of node v_i can be denoted as $N(v_i) = \{v_j \,|(v_i, v_j) \in E\}$.

Definition 5. Adjacency Matrix. The adjacency matrix can be used to represent a finite graph, which is the form of a mathematical matrix and is defined as $A \in \mathbb{R}^{N \times N}$. There is $A_{i,j} = 0$ if $e = (v_i, v_j) \notin E$ and $A_{i,j} = c > 0$ if $e = (v_i, v_j) \in E$ of weighted graph.

2.2 Problem Statement

Given the observed values of M_1 meteorological variables in S weather stations at time step t, for $t = 1, 2, \cdots, \mathcal{P}$, we consider it as the set of spatio-temporal hierarchical graphs, denoted as $\mathcal{X} = \{\mathcal{G}^1, \mathcal{G}^2, \cdots, \mathcal{G}^{\mathcal{P}}\}$. In this graph, observed value is seen as the feature of corresponding node. More generally, the auxiliary feature also can be coupled with primary observed value such as station ID and time of the day, etc. Under this circumstance, $W_t \in \mathbb{R}^C$ where C is the feature dimension. The ground truth of target meteorological variables over future $\mathcal{Q}$ time steps for all stations denoted as $\mathcal{Y} = \{\mathcal{G}^{\mathcal{P}+1}, \mathcal{G}^{\mathcal{P}+2}, \cdots, \mathcal{G}^{\mathcal{P}+\mathcal{Q}}\}$. Our goal is to build model for discovering the hidden mapping from $\mathcal{X}$ to $\mathcal{Y}$.

3 METHODOLOGY

In this section, we first introduce the network architecture of Hierarchical Spatio-Temporal Graph Neural Network. Then we describe each component in details.

3.1 Network Architecture

As shown in Figure 3, HiSTGNN adopts hierarchical and iterative architecture to extract spatio-temporal features of local station as well as across stations. It principally consists of *adaptive graph learning layer*, *spatio-temporal learning module* and *dynamic interaction learning module*. To discover the implicit correlation among meteorological variables and among weather stations, adaptive graph learning module constructs self-learning local graphs and the global graph in the form of graph adjacency matrix and them are later fed into graph neural networks. Spatio-temporal learning module is composed of graph convolutional network and temporal convolutional network with dilated inception to capture spatial and temporal dependencies. With the purpose of building the bidirectional information passing between two level graphs, the dynamic interaction learning module is divided into *information fusion layer* and *information diffusion layer*, which are interleaved with the spatio-temporal learning module of local graphs and global graph. The more details of HiSTGNN are introduced as follows.

3.2 Adaptive Graph Learning Layer

For capturing the hidden association among meteorological variables and among weather stations, we design a hierarchical graph, which is intuitive to indicate the inter-variable and inter-station relations. The key to build this graph is to measure the relation between paired nodes of variable-level and station-level graph (i.e., graph structure). The most existing studies rely on pre-defined graph, such as Euclidean distance, Pearson correlation coefficient [21]. However, in weather forecasting domain, such relation is complex and implicit due to coupled meteorological variables and the geographical correlation between paired stations. Under this circumstance, we desire that relation can be learned from observed data.

To construct adaptive graph, existing methods mainly adopt node embedding and dot production to calculate the similarity between nodes. In this way, learned adjacency matrix is a symmetric matrix and can be seen as an undirected graph. According meteorology theory, we argue that the relation between meteorological variables should be unidirected as they affect each other and to different degrees, which is similar to the change on one road segment's traffic flow causes the change on another road segment [17]. Inspired by these, we propose adaptive graph learning (AGL) layer to learn dynamically adjusted and uni-directed adjacency matrices of local graphs and the global graph. Specifically, AGL can be formulated as follows,

$$A = ReLU(F(\mathcal{M})), \tag{1}$$

$$F = tanh(\alpha \cdot), \tag{2}$$

$$\mathcal{M} = \mathcal{M}_1 \mathcal{M}_2^T - \mathcal{M}_2 \mathcal{M}_1^T, \tag{3}$$

$$\mathcal{M}_1 = F(E_1 \mathcal{W}_1), \mathcal{M}_2 = F(E_2 \mathcal{W}_2), \tag{4}$$

where $\mathcal{W}_1$ and $\mathcal{W}_2$ are linear transformation parameters, E_1 and E_2 are node embedding matrices randomly initialized and are continuously optimized during training. F is tanh activation function with α parameter to control saturation. $\mathcal{M}$ is the skew-symmetric matrix, thus $-\mathcal{M}$ is equal to $\mathcal{M}^T$ and the diagonal variables are zero. The A turns to asymmetric matrix when $\mathcal{M}$ passes through the linear rectification unit.

We construct local graphs and global graph, respectively, denoted as $A = \{A_l^1, A_l^2, \cdots, A_l^S, A_g\}$. And they are later transported to the spatial learning to guide the node feature updating by aggregating neighbor information.

3.3 Spatial Temporal Learning Module

In this subsection, we introduce the Spatial Temporal Learning (STL) module to capture temporal pattern and spatial dependencies among weather stations and among meteorological variables. The STL mainly consists of two components: Gate Temporal Convolution and Spatial Graph Convolution whose details are described as follows.

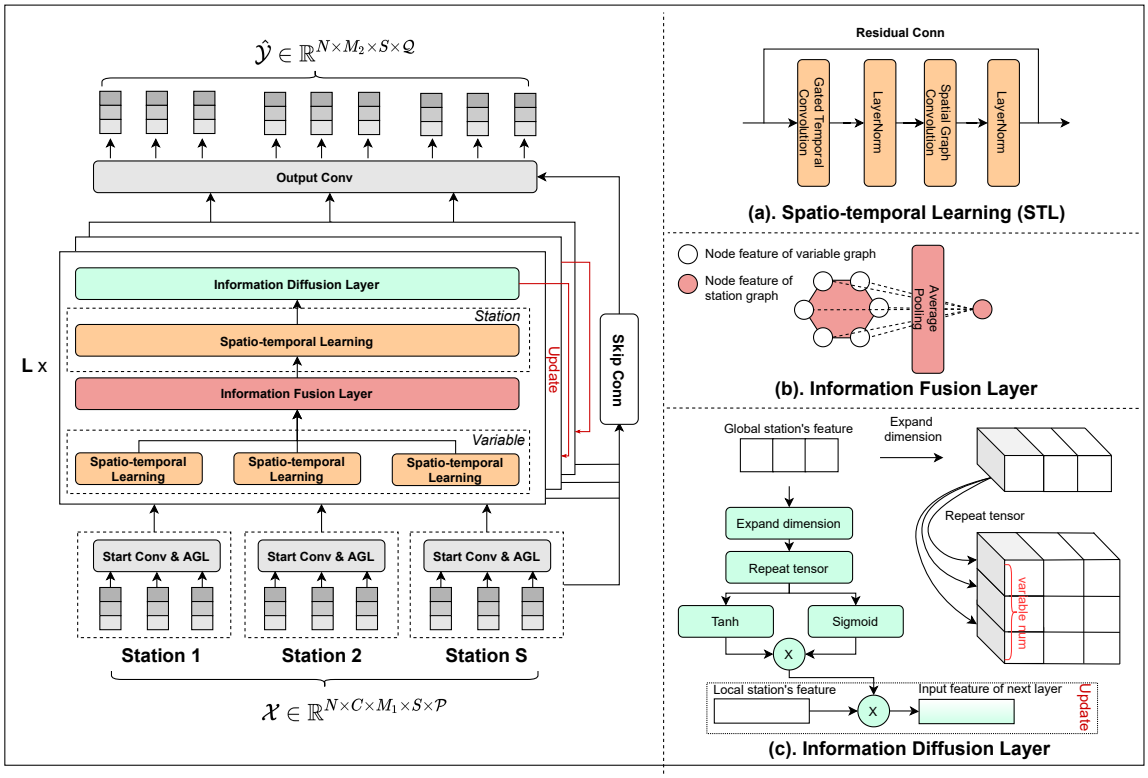

Fig. 3. The framework of HiSTGNN. The start conv is a 1×1×1 standard convolution to project the inputs to latent space. AGL is the adaptive graph learning layer to generate the adjacency matrix of both local graphs and the global graph denoted as A^l and A^g respectively. STL is the spatio-temporal learning module to capture spatio-temporal dependencies. The information fusion layer and information diffusion layer are used to build interactions between two level graphs and between adjacent network layers. The output conv is a 1×d×1 standard convolution to output desired meteorological variables and future steps. The hyper-parameter L represents the number of stacked layers.

3.3.1 Gated Temporal Convolution

The gated temporal convolution aims to capture temporal patterns with long sequences and multi-scale time ranges, following the time axis of hierarchical spatio-temporal graph. To discover temporal pattern, RNN-based networks, relying on the native recursive manner, are suitable for modeling sequential features. However, such mechanism also makes that current state is limited by the previous state and increases the time-consuming costs. The dilated CNN [23] defines a dilation factor to indicate the number of steps skipped in standard convolution operation, which can exponentially expand the receptive field to handle the long sequences. Mathematically, assuming the dilated convolution with k layers of kernel size c and dilation factor exponentially increasing by rate d ($d > 1$) for each layer, the size of receptive filed can be represented as

$$RF^k = 1 + (c-1)(d^k - 1)/(d-1). \tag{5}$$

Therefore, it do not increase the scale of model parameter to capture much long sequences, compared to the canonical convolution. Moreover, the inception network as the backbone of GoogLeNet [24], achieves competitive performance in computing vision by concatenating several outputs of convolution with different filter kernel sizes. Inspired by the dilated CNN and inception, we employ dilated inception as the basic unit of gated temporal convolution to model long and various temporal dependencies. Given the transformed high-dimensional feature after start convolution X, the output of dilated inception can be defined as follows,

$$Z_{\mathcal{T}} = concat(f^d_{1\times c_1}(X), f^d_{1\times c_2}(X), \cdots, f^d_{1\times c_h}(X)) \tag{6}$$

where f represents convolutional function, d is dilation factor, h and c_h denotes the number of kernel and corresponding kernel size.

Moreover, for controlling the information passing to next layer, GTC adopts gated activation unit which integrates two dilated inception layer as the final temporal output represented as follows,

$$\mathbb{Z}_{\mathcal{T}} = tanh(Z_{\mathcal{T}}) \odot sigmoid(Z_{\mathcal{T}}) \tag{7}$$

where $tanh$ and $sigmoid$ are tangent hyperbolic activation function and sigmoid activation function respectively, $\odot$ is hadamard product, $Z_{\mathcal{T}}$ is the output of temporal convolution. In this way, the temporal features of local graphs and the global graph can be denoted as $\mathbb{Z}^l_{\mathcal{T}} = \{\mathbb{Z}^l_{\mathcal{T},1}, \mathbb{Z}^l_{\mathcal{T},2}, \cdots, \mathbb{Z}^l_{\mathcal{T},S}\}$ and $\mathbb{Z}^g_{\mathcal{T}}$.

3.3.2 Spatial Graph Convolution

After capturing the temporal pattern, we propose Spatial Graph Convolution (SGC) to model the spatial feature of local graph/global graph, which consists of two graph convolution layers to handle bidirectional information of uni-directional graph. Based on self-learning graph, the graph convolution learns node representation with graph structural information by aggregating the features of neighborhood. First, we give the mathematical form of the graph

convolution layer. Its layer-wise propagation rule can be defined as follows,

$$H^{(l+1)} = \beta H_{in} + (1-\beta) L_{rm} H^{(l)}, \tag{8}$$

$$L_{rm} = \widetilde{D}^{-1}\widetilde{A}. \tag{9}$$

Here L_{rm} is the random walk normalized laplacian, $\widetilde{A} = A + I$ is the adjacency matrix with self-connections, I is the identity matrix, $\widetilde{D} = \sum_j \widetilde{A}_{ij}$ is the degree matrix, β is a hyperparameter, H_{in} represents the original nodes' states (i.e., $\mathbb{Z}_{\mathcal{T}}$). The motivation using the above propagation rule includes two points: 1). L_{rm} not L_{sym} [25] is suitable for uni-directional adaptive graph with asymmetric matrix. 2). The node hidden states converge to a single point following the number of graph convolution layer approach infinity. To avoid this, β is designed to control the ratio of the original node's information in per message propagation layer.

To further capture the information diversities between different layers, we utilize $\mathcal{W}$ parameter weight to filter information which can be represented as follows,

$$Z_{\mathcal{S}} = \sum_{i=0}^{K} H^i \mathcal{W}^i \tag{10}$$

Here, K is the depth of Spatial Graph Convolution. Finally, consider the inflow information and outflow information of each node, we combine two graph convolution layers to represent the final spatial feature. It is formulated as follows,

$$\mathbb{Z}_{\mathcal{S}} = Z_{\mathcal{S}}^{A} + Z_{\mathcal{S}}^{A^T} \tag{11}$$

In this way, the spatial features of local graphs and global graph can be denoted as $\mathbb{Z}^l_{\mathcal{S}} = \{\mathbb{Z}^l_{\mathcal{S},1}, \mathbb{Z}^l_{\mathcal{S},2}, \cdots, \mathbb{Z}^l_{\mathcal{S},S}\}$ and $\mathbb{Z}^g_{\mathcal{S}}$.

3.4 Dynamic Interaction Learning Module

For modeling the interaction of spatio-temporal features between local graphs and the global graph, we propose the dynamic interaction learning module, which casts the information passing between two level graphs as the fusion process and the diffusion process. To this end, the dynamic interaction learning module consists of an information fusion layer and information diffusion layer correspond to the above processes respectively. As shown in Figure 3, they are interleaved with the spatio-temporal learning module of the local graph and global graph and dynamically capture the feature representation of both graphs.

Information Fusion Layer. We regard observed data of meteorological variables as the node's initial status of each local graph due to the global graph without explicit observed data. The simple but effective strategy is to fusing the nodes' information of the corresponding weather station as the node's hidden status of the global graph. In this paper, we adopt the average pooling to aggregate nodes' hidden representation. The information fusion of k^{th} layer of network can be formulated as follows,

$$\mathbb{Z}^l_{\mathcal{S},k} = ST^l(\mathbb{Z}^l_{\mathcal{S},k-1}) \tag{12}$$

$$\mathbb{Z}^g_{\mathcal{S},k} = ST^g(\frac{1}{S}\sum_{i=0}^{S} \mathbb{Z}^l_{\mathcal{S},k-1,i}) \tag{13}$$

where ST^l represents the local-level spatio-temporal learning operation and ST^g corresponds to the global one, S is the number of weather stations.

Information Diffusion Layer. The information diffusion aims to transfer the global graph's spatial temporal feature to local graphs. Due to the dimension gap between $\mathbb{Z}^l_{\mathcal{S}}$ and $\mathbb{Z}^g_{\mathcal{S}}$, we first expand the dimension of variable by inserting a new axis and fill it by repeating the station dimension value M_1 times. Then, we employ the gate mechanism to control the amount of information passing to the local graphs. The mathematical form of information diffusion operation can be represented as follows,

$$\mathbb{Z}'^g_{\mathcal{S},k} = \mathbb{Z}^g_{\mathcal{S},k} \otimes M_1 \tag{14}$$

$$\mathbb{Z}'^l_{\mathcal{S},k} = tanh(\mathbb{Z}'^g_{\mathcal{S},k}) \odot sigmoid(\mathbb{Z}'^g_{\mathcal{S},k}) \odot \mathbb{Z}^l_{\mathcal{S},k} \tag{15}$$

here $\otimes$ denotes tensor repetition. $\mathbb{Z}'^l_{\mathcal{S},k}$ is fed into the next layer as the updated local graph features.

3.5 Learning Algorithm

Except for above modules, the output module consists of two 3D standard convolutional layers with kernel filter size $1 \times 1 \times 1$ and $1 \times d \times 1$ where $d = M_1 + 1 - M_2$. Besides, we set the number of output channels of the last layer as a factor of the step size $\mathcal{Q}$ which directly outputs our desired time dimension instead of recursively generating $\hat{\mathcal{Y}}$ on the $\mathcal{Q}$ steps. After obtaining the predicted results $\hat{\mathcal{Y}} = \{\hat{y}^{\mathcal{P}+1}, \hat{y}^{\mathcal{P}+2}, \cdots, \hat{y}^{\mathcal{P}+\mathcal{Q}}\}$, we adopt the mean absolute error (MAE) as the loss function of HiSTGNN, which is defined as follows,

$$L(\mathcal{X};\Theta) = \frac{1}{NSM_2\mathcal{Q}} \sum_{i=1}^{N}\sum_{j=1}^{S}\sum_{q=1}^{M_2}\sum_{t=\mathcal{P}+1}^{\mathcal{Q}} |\hat{y}_{i,j,q,t} - y_{i,j,q,t}| \tag{16}$$

We optimize the parameters by minimizing the loss function of mini-batch samples with an Adam optimizer [26]. Covering all procedures, our algorithm is given in Algorithm 1.

4 Experiments

In this section, we validate the effectiveness of proposed HiSTGNN on three real-world weather datasets. First, we introduce the relevant experimental settings, including datasets, evaluation metrics, comparison methods and hyper-parameter settings. Then we give the experimental results and analysis in detail.

4.1 Experimental Settings

4.1.1 Datasets

We conduct experiments on three real-world weather datasets (WDs) as shown in TABLE 1, detailed as follows.

- *WD_BJ*[1]*:* The weather dataset is collected by 10 automatic weather stations (AWSs) in Beijing. For each station, it generates 9 meteorological variables such as temperature at 2 meters (t2m), relative humidity at 2 meters (rh2m), wind at 10 meters (w10m), and et

1. https://github.com/BruceBinBoxing/Deep_Learning_Weather_Forecasting

Algorithm 1 Hierarchical Spatio-temporal Graph Neural Network for Weather Forecasting

Input: $\mathcal{X} \in \mathbb{R}^{B\times C\times S\times M_1\times \mathcal{P}}$: The batch input of the observed multiple stations and multiple meteorological variables time series data; L: The number of layers;
Output: $\hat{\mathcal{Y}} \in \mathbb{R}^{B\times C\times S\times M_2\times \mathcal{Q}}$

$A^l_{adp} = ADL(M_1)$; $A^g_{adp} = ADL(S)$
$X^1 = start\_conv(\mathcal{X})$; $skip = skip\_conv(\mathcal{X})$
for each $k \in [1, L]$ **do**
  $residual = X^k$; $stat\_x = []$; $skip\_x = []$
  for each $j \in [1, S]$ **do**
    $\mathbb{Z}^l_{\mathcal{T},j} = GTC(X^k[:,:,j,:,:])$
    $skip\_x[j] = LayerNorm(\mathbb{Z}^l_{\mathcal{T},j})$
    $\mathbb{Z}^l_{\mathcal{S},j} = SGC(skip\_x[j], A^l_{adp,j})$
    $stat\_x[j] = LayerNorm(\mathbb{Z}^l_{\mathcal{S},j})$
  end for
  $skip = skip + skip\_conv(skip\_x)$
  $X^k_g = avg\_pool(stat\_x)$
  $\mathbb{Z}^g_{\mathcal{T}} = GTC(X^k_g)$
  $\mathbb{Z}^g_{\mathcal{S}} = LayerNorm(SGC(LayerNorm(\mathbb{Z}^g_{\mathcal{T}}), A^g_{adp}))$
  $X^{k+1} = (tanh(\mathbb{Z}^g_{\mathcal{S}}) \odot sigmoid(\mathbb{Z}^g_{\mathcal{S}})) \odot X^k$
end for
$skip = skip\_conv(X^L) + skip$
$\hat{\mathcal{Y}} = end\_conv2(ReLU(end\_conv1(ReLU(skip))))$

al. Following the pre-processing by [5], we use linear interpolation along temporal dimension to impute missing values and use min-max normalization to normalize each variable. Following [5], we also choose t2m, rh2m, w10m as the target variables and sequentially split the dataset into training set, validation set and test set from 1st Mar. 2015 - 31th May. 2018, 1st June. 2018 - 28th Aug. 2018, 29th Aug. 2018 - 3rd Nov. 2018, respectively.

- *WD_ISR*[2]*:* The weather dataset is acquired from OpenWeather[3] and contains 6 cities of Israel, each of which generates four meteorological variables: temperature, humidity, wind speed and atmospheric pressure. We adopt the same data pre-processing as WD_BJ dataset, and make four variables as predicted targets. As for the data partition, We choose last 10 percent of data as test set, former 80 percent of data as training set, remaining data as validation set.
- *WD_USA*[2]*:* Except that it is observed from 13 cities in the United States of America, the weather dataset's setup identical to WD_ISR.

4.1.2 Evaluation Metrics

We measure our method and baselines by two common deviation-based evaluation metrics: Root Mean Squared Error (RMSE) and Mean Absolute Error (MAE) as

$$RMSE = \sqrt{\frac{1}{n}\sum_i (y_i - \hat{y}_i)^2}, MAE = \frac{1}{n}\sum_i |y_i - \hat{y}_i|,$$

2. https://www.kaggle.com/selfishgene/historical-hourly-weather-data
3. https://home.openweathermap.org/

TABLE 1
Data statistics.

Data	WD_BJ	WD_ISR	WD_USA
Location	Beijing	Iseral	United States of America
Time span	3/1/2015-10/15/2018	10/2/2012-10/28/2017	10/2/2012-10/28/2017
Time interval	1 hour	1 hour	1 hour
Meteorological variable	9	4	4
Weather station	10	6	13
Sample size	1301	1850	1850
Input length ($\mathcal{P}$)	28	48	48
Output length ($\mathcal{Q}$)	33	24	24

where y and $\hat{y}$ are the ground truth and the predicted values; n is the number of all available predicted values. For them, lower values are better. As same with DUQ [5], we first calculate the performance of each target variable over all time steps, then take the average of the corresponding one as the ultimate RMSE and MAE criterion.

4.1.3 Baselines

We compare our HiSTGNN with the following 7 baselines:

- SARIMA [9]: Seasonal Autoregressive Integrated Moving Average where we predicted each target variable, respectively, as univarate time series forecasting.
- SVR [27]: Support Vector Regression that is a variant of support vector machine for regression.
- Seq2Seq [28]: Sequence to Sequence model in which we selected gated recurrent units as the backbone network of encoder and decoder with two layers and 300 hidden units of each layer to predict the next step, iteratively.
- WaveNet [22]: A convolutional neural model with stacking multiple dilated casual convolutions for sequence task.
- DUQ [5]: A deep uncertainty quantification method, showing state-of-the-art performance on weather forecasting.
- AGCRN [18]: Adaptive Graph Convolutional Recurrent Network, which combines graph convoluitonal neural network and recurrent neural network. Here, we took each station as node and corresponding meteorological variables as node's features.
- MTGNN [17]: A state-of-the-art model for multivariate time series forecasting. The setting is same as AGCRN.

4.1.4 Hyperparameter Settings

Here, we introduce the hyperparameter settings of our HiSTGNN. The common parameters include: learning rate, batch size and training epoch. By default, we set learning rate to 0.001, batch size to 32 and training epoch to 100. Besides, we set the number of layers to 3, the depth of GNN to 2 both for local and global graph learning. For convolution units, the input and output channels of 1x1 start convolution are set to 2 and 32. The dilated inception is set to 32 channels for input and output. Afterwards, we use dropout with 0.3 rate and layer normalization after

TABLE 2
Performance comparisons with baselines on three weather datasets.

Datasets		WD_BJ				WD_ISR					WD_USA				
Methods	Metrics	TEMP	HUM	WIND	**Avg.**	TEMP	HUM	WIND	PSUR	**Avg.**	TEMP	HUM	WIND	PSUR	**Avg.**
SARIMA	MAE	2.4217	14.3882	1.1503	5.9867	3.1419	15.8560	1.3799	3.6863	6.0160	2.3112	11.6933	1.4677	3.2208	4.6732
	RMSE	3.3216	19.6555	1.6459	8.2077	4.0347	19.2929	1.7756	6.2767	7.8450	3.1213	15.9734	2.0920	4.4713	6.4370
SVR	MAE	2.0457	11.3279	0.8727	4.7488	2.0735	7.5681	**0.8843**	13.0304	5.8891	1.8623	9.5281	1.2035	5.6109	4.5512
	RMSE	2.7901	15.5308	1.2655	6.5288	2.0735	11.3228	1.2992	22.5605	9.3670	2.6075	12.7102	1.6492	8.0626	6.2574
Seq2Seq	MAE	2.0259	10.8049	0.8954	4.5754	1.3726	7.9663	0.9140	2.7346	3.2469	1.7599	9.3221	**1.1497**	2.1196	3.5878
	RMSE	2.6985	14.7942	**1.2443**	6.2457	1.8923	11.9565	1.3261	5.3360	5.1277	2.4765	12.2728	1.6016	3.0579	4.8522
WaveNet	MAE	2.2591	10.9460	1.0051	4.7368	1.5107	7.4604	0.9601	2.7631	3.1796	1.9139	9.4432	1.2654	2.0311	3.6634
	RMSE	2.9978	15.1380	1.3396	6.4918	1.9306	**10.5613**	1.3683	4.2814	**4.5405**	2.6709	12.5661	1.6851	2.9163	4.9596
DUQ	MAE	2.0221	10.2879	0.8801	4.3967	1.3487	8.0896	0.9213	3.0548	3.3536	1.9424	9.8207	1.1663	2.4250	3.8386
	RMSE	2.7343	14.9173	1.2702	6.3072	1.8748	11.2739	1.3186	5.1690	4.9091	2.6363	12.4793	**1.5862**	3.4099	5.0279
MTGNN	MAE	2.0181	10.3525	0.8684	4.4130	1.4483	7.5238	1.0138	2.5149	3.1252	1.8201	**9.1287**	1.1749	2.2735	3.5993
	RMSE	2.7186	14.9944	1.2596	6.3242	1.9290	10.8361	1.4185	4.2898	4.6184	2.4732	12.2703	1.5930	3.0508	4.8468
AGCRN	MAE	**1.8912**	10.5406	0.8932	4.4416	1.2644	7.5966	0.9000	2.5471	3.0770	1.9040	9.2218	1.2746	**1.9605**	3.5902
	RMSE	**2.6270**	14.9901	1.2576	6.2916	**1.7261**	11.3350	**1.2769**	4.6245	4.7406	2.5505	12.3767	1.8039	**2.9023**	4.9083
HiSTGNN(our)	MAE	1.9533	**9.8089**	**0.8671**	**4.2098**	**1.2551**	**7.2302**	0.9807	**2.3911**	**2.9643**	**1.7546**	12.2703	1.1760	2.0975	**3.5419**
	RMSE	2.6353	**14.0129**	1.2634	**5.9705**	1.7287	10.9434	1.3753	**4.2666**	4.5785	**2.4247**	**12.2222**	1.6120	2.9052	**4.7910**

each component of the spatio-temporal learning module. We train model by Adam optimizer with gradient clip 5 and l2 regularization penalty 0.0001.

4.2 Main Results

TABLE 2 presents the experimental results of HiSTGNN and compared methods on WD_BJ, WD_ISR and WD_USA data, including the MAE and RMSE of on each variable and the average. We can observe that, HiSTGNN achieves the best performance on most of the tasks and outperforms all other baselines on the average metric, except for the RMSE with 0.8% degradation compared with the top on WD_ISR data. In particular, we note that HiSTGNN shows 4.25% and 5.34% improvements in terms of MAE and RMSE on WD_BJ data, compared to state-of-the-art weather forecasting method, i.e., DUQ. In general, there are a total of 28 instances for each method in which the graph-based methods (i.e., HiSTGNN, MTGNN and AGCRN) gain top performance with 22 counts while the univariate time series forecasting methods (i.e., SARIMA and SVR) get 1 best instances. A reasonable explanation is that promotion is benefited from the effectiveness of handling spatial features since the above some target variables with weak seasonal variation and no seasonal variation are difficult to capture temporal features. Taking the temperature, relative humidity and pressure of New York on WD_USA data as example, only the temperature presents a strong seasonal variation, relative humidity and pressure are under much noise (see Fig. 4). Among graph-based methods, HiSTGNN achieve 14 best performance compared with others using flat graph (only variable-level graph), which demonstrates the effectiveness of hierarchical graph structure.

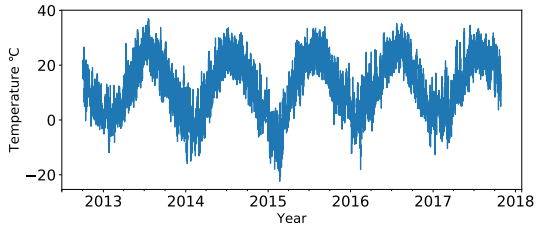

(a) Temperature

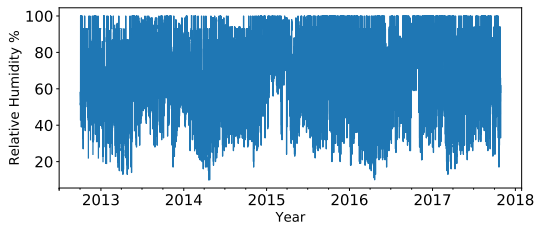

(b) Relative humidity

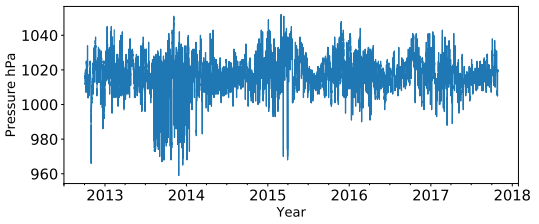

(c) Pressure

Fig. 4. The time series data visualization on three target variable in New York from 02/10/2012-10/28/2017.

4.3 Study of the Dynamic Interaction Learning

In this section, we conduct experiments on variants of HiSTGNN to validate the effectiveness of proposed dynamic interaction learning module. For building the connection between different weather stations, we introduce the information fusion and diffusion mechanism in dynamic manner in Section 3.4 where there are three aspects need to note: 1). interaction type, including following ways:

TABLE 3
Comparison on WD_BJ test set with variants of dynamic interaction.

Interaction type	Fusion	Diffusion	MAE	RMSE
DI	Avg Pool	Gate	**4.2098±0.0568**	**5.9705±0.0769**
DI	Max Pool	Gate	4.3743±0.0997	6.0537±0.1244
DI	Avg Pool	w/o	4.3545±0.0812	6.0268±0.1061
DI	Max Pool	w/o	4.3641±0.0923	6.0238±0.1079
w/o DI	-	-	4.5321±0.0587	6.2003±0.0602
OSI	Avg Pool	Gate	4.4351±0.0524	6.1520±0.0771
OSI	Max Pool	Gate	4.4371±0.0426	6.1514±0.0437
OSI	Avg Pool	w/o	4.4729±0.0515	6.1872±0.0678
OSI	Max Pool	w/o	4.4404±0.0390	6.1707±0.0821

- **DI**: HiSTGNN following iterative interaction with multi-layer stacking network.
- **OSI**: HiSTGNN with one-shot interaction where we replace the interaction between local graphs and the global graph in per layer with only one fusion and diffusion operation at the beginning and the end.
- **w/o DI**: HiSTGNN without hierarchical graph structure in which we remove the related components of global graph on temporal and spatial learning.

2). fusion with average pooling or max pooling. 3) diffusion with gate mechanism or w/o. Hence, there are 9 variants in total as shown in TABLE 3. We repeat per experiment 10 times with the same parameters for all variants and report the average of MAE and RMSE and the standard deviation. From the table, we can find that *dynamic interaction + average pooling + gate* outperforms other variants. In detail, DL is better than OSI among three interaction types. OSI is superior to w/o DI whereas the latter is still competitive compared to baselines. Besides, the variants of diffusion has an outstanding impact on performance than ones of fusion. A reason may be that the gate mechanism makes more effect on information propagation than the diversity between average pooling and max pooling.

4.4 Study of Adaptive Graph Learning

To demonstrate the effectiveness of adaptive graph learning, we first compare following three ways of building graph adjacency matrix A: 1). Predefined A, calculated by correlation coefficient matrix; 2). Undirected A, computed by similarity of node embedding and denoted as $A = softmax(ReLU(EE^T))$; 3). Directed A same with undirected A but with two node embedding and denoted as $A = softmax(ReLU(E_1E_2^T))$. Fig. 5 illustrates that unidirected graph adjacency achieves the lowest MAE and RMSE. It outperforms over predefined A and undirected A significantly. With the same directed structure, directed A lower than our method marginally, especially in the terms of MAE.

We next conduct a case study to investigate whether the learned local graphs and global graph. As shown in Fig. 6(a), we visualize the weather stations of the WD_USA data and highlight Philadelphia and its three neighbors with highest weights which are New York, Boston and Detroit, respectively. Philadelphia and New York are geographically

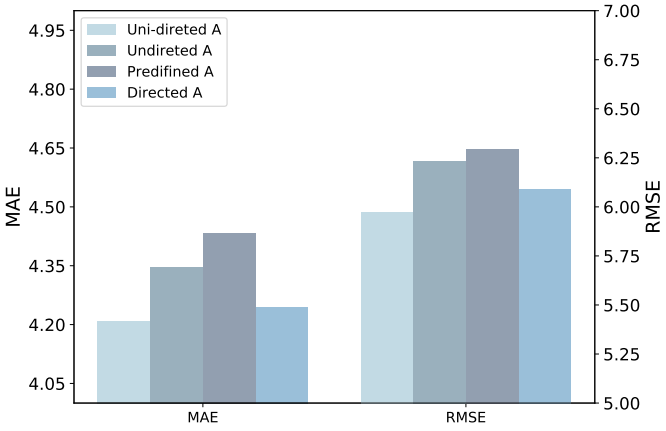

Fig. 5. The performance on four types of graph adjacency matrix in WD_BJ test set.

(a) The Philadelphia node with its top-3 neighbors in adjacency matrix of adaptive graph learning

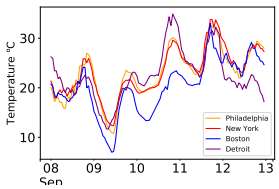

(b) Temperature trends of four cities from 8th Sep. to 12th Sep. 2013

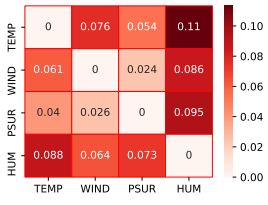

(c) The learned edge weights among variables on WD_USA test set

Fig. 6. Case study

similar both with temperate continental climate, so have the highest correlation. Boston and Philadelphia, although spatially distant from each other, are both influenced by ocean currents and locate in climatic zone. Fig. 6(b) depicts four cities' temperature change range from 8th Sep. to 12th Sep. 2013 in which the temperature change follows similar trend, despite there are some gaps among them. Furthermore, we plot the mean edge weights among variables of 13 stations by heat map, shown in Fig. 6(c). We can observe the relationship between relative humidity and temperature, atmospheric pressure and wind speed decreases sequentially, which is in accordance with meteorological theory. And the correlation coefficients are all relatively small due to the complexity of the meteorological factor associations.

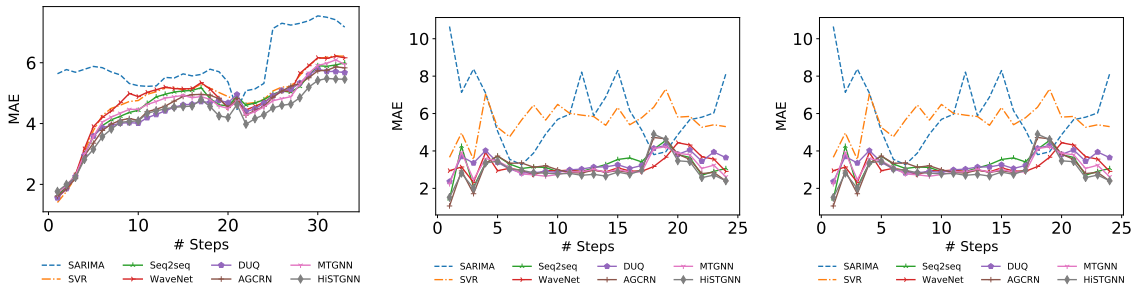

(a) MAE on WD_BJ test set (b) MAE on WD_ISR test set (c) MAE on WD_USA test set

Fig. 7. MAE on three weather datasets with baselines over multiple time steps

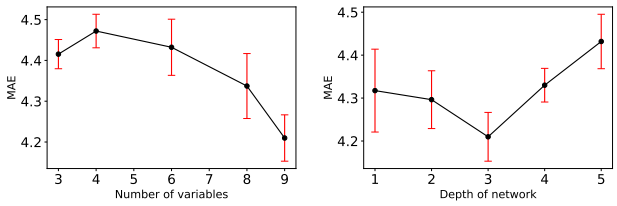

(a) Number of variables (b) Depth of network

Fig. 8. Effect of graph size and network depth on WD_BJ data

4.5 Study of Model Parameters

4.5.1 *Effect of graph size*

To further explore the effectiveness of graph scale for weather forecasting model, we select different number of meteorological variable with [3, 4, 6, 8, 9] from WD_BJ data and use 10-station for all cases. Fig. 8(a) illustrates that prediction performance gradually increases as the variable-level graph expands. The study of scale boundaries of the variable-level graph is not supported due to the limitation of the number of meteorological variables, The reason why we not conduct experiment on different number of weather station is mainly due to the inherent variation in the prediction performance of stations thus the ultimate results are affected not only by the capability of global graph learning with different size, but also by the bias among stations.

4.5.2 *Effect of network depth*

Fig. 8(b) presents the influence of network depth on WD_BJ data. Deeper network expands the spatio-temporal receptive field and enhances our model's representation capability. However, As network grows much deeper, the network training process turns into much more difficult, resulting in the MAE gradually increases.

4.6 Multi-step Forecasting

In this section, we further explore the multi-step forecasting capability of HiSTGNN and baselines. As shown in Figure 7, we can observe that NN-based methods consistently outperform statistical machine learning methods. HiSTGNN, specially, achieves best performance on all datasets over most of multiple time steps which showed as that a diamond-shaped gray line is under the other lines. We also noted that MAE gradually raises following the time step increase, which is consistent with the principle of multi-step forecasting, i.e., the uncertainty grows over time (shown in Fig. 7(a)). However, there is also the possibility that predictions are more likely to be accurate at a given point in time, due to the periodic changes of time series (shown in Fig. 7(b) and Fig. 7(c)).

5 Related Work

5.1 Weather Forecasting

Accurate and timely weather forecasting plays an important role in human livelihood. The widely used method is numerical weather prediction [3], [7], [8]. However, this method suffers from the issues of high computing complexity and unstable modeling under inappropriate initial solution. Recently, with the increase of meteorological data, researchers cast weather forecasting as spatio-temporal forecasting task from the machine learning perspective. Early works mainly employ traditional machine learning methods such as ARIMA [9], SVM [10] to capture the temporal pattern of a few variables, which lacks the modeling relationships among meteorological variables. More recently, some deep learning-based methods have shown a great advantage in the field of weather forecasting. A hybrid weather forecasting method [11] was proposed to model the mutual influence among meteorological variables. Combining CNNs and LSTM, ConvLSTM [12] was proposed to capture spatio-temporal correlation between meteorological variables simultaneously to predict precipitation. The study in [5] designed a novel loss function to predict the sequential point and prediction interval from the viewing of uncertainty quantification. However, these methods either neglect the spatial dependencies between weather stations or lack explicit modeling of spatio-temporal information interactions.

5.2 Spatio-temporal Graph Neural Networks

Recently, many studies focus on applying spatio-temporal graph neural networks in spatio-temporal forecasting tasks like traffic prediction [13], taxi demand prediction [14], driver maneuver anticipation [15] and air quality analysis [16], in which graph convolution was to capture spatial dependence following the given graph structure and RNNs or CNNs was to model temporal dependence. Apart from the pre-defined graph used in the above works, In studies [17], [18], the spatio-temporal learning based on graph data

was generalized to a multivariate time series forecasting paradigm by proposing a parametric graph structure adaptively learned from raw data. However, to the best of our knowledge, spatio-temporal graph neural networks are no relevant exploration in multi-station weather forecasting.

5.3 Hierarchical Graph Neural Networks

A major constraint of current GNNs is that their architectures are flat so as not to aggregate information in a hierarchical way. To solve this issue, a hierarchical graph neural network [19] was proposed for the node classification task, which generates hierarchical representations of a graph by pooling operation. Besides, in study [20], they cast road networks and region networks as a hierarchical graph and adopted hierarchical graph convolution networks to model spatial correlation, for traffic forecasting. However, the above work either lacks information transfer from top to bottom or from bottom to top, which may causes some information to be lost. Unlike the previous methods, our approach learns adaptive graphs in an end-to-end fashion and builds bidirectional information passing between the variable-level graph and station-level graph.

6 Conclusion

In this paper, we proposed a Hierarchical Spatio-Temporal Graph Neural Networks (HiSTGNN) framework to capture spatio-temporal dependencies of multiple weather stations and multiple meteorological variables simultaneously in an end-to-end way. HiSTGNN first constructs adjusted dependency matrices of the local graphs and the global graph by an adaptive graph learning layer. Then it employs spatio-temporal learning modules to model spatial and temporal dependencies. It further designs a dynamic interaction learning module to aggregate the representation of the local graph into the corresponding global node, and diffuse information in an inverse direction, respectively.

The experimental results showed our method achieved state-of-the-art performance on three real-world meteorological datasets. Further analysis on graph scale revealed forecasting accuracy is vulnerable to its influence, which prompted us to focus on the large-scale meteorological data with much more meteorological variables and stations in future research.

Acknowledgment

This research was supported by the National Key R&D Program of China (2019YFB2101802) and the National Natural Science Foundation of China (No. 61773324).

References

[1] T. Gneiting and A. E. Raftery, "Weather forecasting with ensemble methods," *Science*, vol. 310, no. 5746, pp. 248–249, 2005.

[2] Y. Zheng, L. Capra, O. Wolfson, and H. Yang, "Urban computing: Concepts, methodologies, and applications," *ACM Trans. Intell. Syst. Technol.*, vol. 5, no. 3, pp. 38:1–38:55, 2014. [Online]. Available: https://doi.org/10.1145/2629592

[3] M. Tolstykh and A. Frolov, "Some current problems in numerical weather prediction," *Izvestiya Atmospheric and Oceanic Physics*, vol. 41, no. 3, pp. 285–295, 2005.

[4] C. K. Sønderby, L. Espeholt, J. Heek, M. Dehghani, A. Oliver, T. Salimans, S. Agrawal, J. Hickey, and N. Kalchbrenner, "Metnet: A neural weather model for precipitation forecasting," *CoRR*, vol. abs/2003.12140, 2020. [Online]. Available: https://arxiv.org/abs/2003.12140

[5] B. Wang, J. Lu, Z. Yan, H. Luo, T. Li, Y. Zheng, and G. Zhang, "Deep uncertainty quantification: A machine learning approach for weather forecasting," in *Proceedings of the 25th ACM SIGKDD International Conference on Knowledge Discovery Data Mining*, 2019, pp. 2087–2095.

[6] P. Hewage, A. Behera, M. Trovati, E. Pereira, M. Ghahremani, F. Palmieri, and Y. Liu, "Temporal convolutional neural (TCN) network for an effective weather forecasting using time-series data from the local weather station," *Soft Comput.*, vol. 24, no. 21, pp. 16 453–16 482, 2020. [Online]. Available: https://doi.org/10.1007/s00500-020-04954-0

[7] G. Marchuk, *Numerical methods in weather prediction*. Elsevier, 2012.

[8] P. Bauer, A. Thorpe, and G. Brunet, "The quiet revolution of numerical weather prediction," *Nature*, vol. 525, no. 7567, pp. 47–55, 2015.

[9] L. Chen and X. Lai, "Comparison between arima and ann models used in short-term wind speed forecasting," in *2011 Asia-Pacific Power and Energy Engineering Conference*. IEEE, 2011, pp. 1–4.

[10] N. I. Sapankevych and R. Sankar, "Time series prediction using support vector machines: a survey," *IEEE Computational Intelligence Magazine*, vol. 4, no. 2, pp. 24–38, 2009.

[11] A. Grover, A. Kapoor, and E. Horvitz, "A deep hybrid model for weather forecasting," in *Proceedings of the 21th ACM SIGKDD International Conference on Knowledge Discovery and Data Mining*, 2015, pp. 379–386.

[12] D. Bahdanau, K. Cho, and Y. Bengio, "Neural machine translation by jointly learning to align and translate," in *3rd International Conference on Learning Representations, ICLR 2015, San Diego, CA, USA, May 7-9, 2015, Conference Track Proceedings*, Y. Bengio and Y. LeCun, Eds., 2015. [Online]. Available: http://arxiv.org/abs/1409.0473

[13] X. Zhang, C. Huang, Y. Xu, L. Xia, P. Dai, L. Bo, J. Zhang, and Y. Zheng, "Traffic flow forecasting with spatial-temporal graph diffusion network," in *Thirty-Fifth AAAI Conference on Artificial Intelligence, AAAI 2021, Thirty-Third Conference on Innovative Applications of Artificial Intelligence, IAAI 2021, The Eleventh Symposium on Educational Advances in Artificial Intelligence, EAAI 2021, Virtual Event, February 2-9, 2021*. AAAI Press, 2021, pp. 15 008–15 015. [Online]. Available: https://ojs.aaai.org/index.php/AAAI/article/view/17761

[14] H. Yao, F. Wu, J. Ke, X. Tang, Y. Jia, S. Lu, P. Gong, J. Ye, and Z. Li, "Deep multi-view spatial-temporal network for taxi demand prediction," in *Proceedings of the Thirty-Second AAAI Conference on Artificial Intelligence, AAAI-18, New Orleans, Louisiana, USA, February 2-7, 2018*, S. A. McIlraith and K. Q. Weinberger, Eds. AAAI Press, 2018, pp. 2588–2595. [Online]. Available: https://www.aaai.org/ocs/index.php/AAAI/AAAI18/paper/view/16069

[15] A. Jain, A. R. Zamir, S. Savarese, and A. Saxena, "Structural-rnn: Deep learning on spatio-temporal graphs," in *2016 IEEE Conference on Computer Vision and Pattern Recognition, CVPR 2016, Las Vegas, NV, USA, June 27-30, 2016*. IEEE Computer Society, 2016, pp. 5308–5317. [Online]. Available: https://doi.org/10.1109/CVPR.2016.573

[16] C. Wang, Y. Zhu, T. Zang, H. Liu, and J. Yu, "Modeling inter-station relationships with attentive temporal graph convolutional network for air quality prediction," in *WSDM '21, The Fourteenth ACM International Conference on Web Search and Data Mining, Virtual Event, Israel, March 8-12, 2021*, L. Lewin-Eytan, D. Carmel, E. Yom-Tov, E. Agichtein, and E. Gabrilovich, Eds. ACM, 2021, pp. 616–634. [Online]. Available: https://doi.org/10.1145/3437963.3441731

[17] Z. Wu, S. Pan, G. Long, J. Jiang, X. Chang, and C. Zhang, "Connecting the dots: Multivariate time series forecasting with graph neural networks," in *Proceedings of the 26th ACM SIGKDD International Conference on Knowledge Discovery Data Mining*, ser. KDD '20. New York, NY, USA: Association for Computing Machinery, 2020, p. 753–763. [Online]. Available: https://doi.org/10.1145/3394486.3403118

[18] L. Bai, L. Yao, C. Li, X. Wang, and C. Wang, "Adaptive graph convolutional recurrent network for traffic forecasting," in *Advances in Neural Information Processing Systems*, H. Larochelle, M. Ranzato, R. Hadsell, M. F. Balcan, and H. Lin, Eds., vol. 33. Curran Associates, Inc., 2020, pp. 17 804–17 815.

[19] Z. Ying, J. You, C. Morris, X. Ren, W. L. Hamilton, and J. Leskovec, "Hierarchical graph representation learning with differentiable pooling," in *Advances in Neural Information Processing Systems 31: Annual Conference on Neural Information Processing Systems 2018, NeurIPS 2018, December 3-8, 2018, Montréal, Canada*, S. Bengio, H. M. Wallach, H. Larochelle, K. Grauman, N. Cesa-Bianchi, and R. Garnett, Eds., 2018, pp. 4805–4815. [Online]. Available: https://proceedings.neurips.cc/paper/2018/hash/e77dbaf6759253c7c6d0efc5690369c7-Abstract.html

[20] K. Guo, Y. Hu, Y. Sun, S. Qian, J. Gao, and B. Yin, "Hierarchical graph convolution networks for traffic forecasting," in *Proceedings of the AAAI Conference on Artificial Intelligence*, vol. 35, no. 1, 2021, pp. 151–159.

[21] J. Chen, L. Liu, H. Wu, J. Zhen, G. Li, and L. Lin, "Physical-virtual collaboration graph network for station-level metro ridership prediction," *arXiv preprint arXiv:2001.04889*, 2020.

[22] A. van den Oord, S. Dieleman, H. Zen, K. Simonyan, O. Vinyals, A. Graves, N. Kalchbrenner, A. W. Senior, and K. Kavukcuoglu, "Wavenet: A generative model for raw audio," in *The 9th ISCA Speech Synthesis Workshop, Sunnyvale, CA, USA, 13-15 September 2016*. ISCA, 2016, p. 125. [Online]. Available: http://www.isca-speech.org/archive/SSW_2016/abstracts/ssw9_DS-4_van_den_Oord.html

[23] F. Yu and V. Koltun, "Multi-scale context aggregation by dilated convolutions," *arXiv preprint arXiv:1511.07122*, 2015.

[24] C. Szegedy, W. Liu, Y. Jia, P. Sermanet, S. Reed, D. Anguelov, D. Erhan, V. Vanhoucke, and A. Rabinovich, "Going deeper with convolutions," in *Proceedings of the IEEE conference on computer vision and pattern recognition*, 2015, pp. 1–9.

[25] T. N. Kipf and M. Welling, "Semi-supervised classification with graph convolutional networks," in *5th International Conference on Learning Representations, ICLR 2017, Toulon, France, April 24-26, 2017, Conference Track Proceedings*, 2017.

[26] D. P. Kingma and J. Ba, "Adam: A method for stochastic optimization," *Proceedings of the International Conference on Learning Representations.*, 2015.

[27] B. Wolff, J. Kühnert, E. Lorenz, O. Kramer, and D. Heinemann, "Comparing support vector regression for pv power forecasting to a physical modeling approach using measurement, numerical weather prediction, and cloud motion data," *Solar Energy*, vol. 135, pp. 197–208, 2016.

[28] I. Sutskever, O. Vinyals, and Q. V. Le, "Sequence to sequence learning with neural networks," in *Advances in Neural Information Processing Systems 27: Annual Conference on Neural Information Processing Systems 2014, December 8-13 2014, Montreal, Quebec, Canada*, Z. Ghahramani, M. Welling, C. Cortes, N. D. Lawrence, and K. Q. Weinberger, Eds., 2014, pp. 3104–3112. [Online]. Available: https://proceedings.neurips.cc/paper/2014/hash/a14ac55a4f27472c5d894ec1c3c743d2-Abstract.html